

## **Sulfur Dioxide Removal in Coal Slurry Reactor**

**Dr. Neran K. Ibrahim\*    Zainab A. Jawad**

**Received on: 23/4/2007**

**Accepted on: 31/1/2008**

### **Abstract**

The objective of this work was to study the feasibility of using coal slurry for the removal of SO<sub>2</sub> from simulated flue gas stream (air, SO<sub>2</sub>). The effect of gas rate, temperature, and initial SO<sub>2</sub> concentration on the overall removal efficiency was investigated at wet and dry bed conditions. The results indicated that the optimum gas rate was 60 ℓ/min. The SO<sub>2</sub> removal efficiency was highly temperature sensitive, and increases with increasing the bed temperature especially at wet bed conditions and decreases with increasing SO<sub>2</sub> initial concentration. A mathematical model for the desulfurization process was proposed based on the material balance for gaseous and solid phase streams. The model was found to give a very good description of the experimental data with 95% confidence level.

**Key words: SO<sub>2</sub> Removal, Coal Slurry Reactor, FGD, Modeling**

---

\* Dept. Chemical Eng., Univ. of Tech.

## 1- Introduction:

Adsorption of sulfur dioxide on carbonaceous materials has been extensively studied. Lizzio and DeBarr <sup>(1)</sup> showed that the reaction of SO<sub>2</sub> with carbon (C) in the presence of O<sub>2</sub> (in air) and H<sub>2</sub>O involves a series of reactions that leads to the formation of sulfuric acid as the final product. The rate-determining step in the overall process is the oxidation of SO<sub>2</sub> to SO<sub>3</sub>. In optimizing the SO<sub>2</sub> removal capabilities of carbon, most studies only assume a given mechanism for SO<sub>2</sub> adsorption and conversion to H<sub>2</sub>SO<sub>4</sub> to be operable. Cho <sup>(2)</sup> reported that activated carbon which contains the catalysis of ferric/ferrous ions for the reaction between SO<sub>2</sub> and O<sub>2</sub> has been known for many years. The oxidation reactions occur by three routes. First, SO<sub>2</sub> serves as a reducing reagent of ferric ion. Second, SO<sub>2</sub> together with O<sub>2</sub> serves as an oxidizing reagent of ferrous ion to ferric ion. Third, ferric ion catalyzes the oxidation reaction of SO<sub>2</sub>. Bagreev *et al.* <sup>(3)</sup> showed that the normalized capacity of the activated carbon adsorbent, especially at higher temperature, is much larger than that of the activated carbon at lower temperature. The significantly higher activity of the surfaces of the adsorbents carbonized at higher temperature result from

the combined effect of dehydroxylation of inorganic phase oxides and their solid state reactions promoted at high temperature and reducing conditions and with increasing temperature new reactive oxides are formed, e.g. FeSO<sub>4</sub> and/or CaSO<sub>3</sub> are well-developed compared to the starting material. Cho and Miller <sup>(4)</sup> studied the overall removal of sulfur dioxide flue gas with coal scrubbing; the objective of the study was to determine the effects of temperature, oxygen concentration and SO<sub>2</sub> concentration on SO<sub>2</sub> removal from simulated flue gas streams and on leaching rate of coal pyrite. Bagreev and Bandosz <sup>(5)</sup> show for the removal of SO<sub>2</sub> using coal slurry the importance of the role of water in the formation of sulfuric acid in pore system. Liu *et al.* <sup>(6)</sup> used waste semi-coke as the raw material to prepare catalysts of industrial scale size for SO<sub>2</sub> removal. The effect of water content in the flue gas, reaction temperature, and space velocity on the de-sulfurizing property was investigated. Space velocity exhibited an optimal value of 830 h<sup>-1</sup>.

The present study focuses on the modeling of the de-sulfurization process in coal slurry reactor.

\* Dept. Chemical Eng., Univ. of Tech.

## 2- Experimental Work:

The experiments were carried out in a laboratory scale apparatus which is shown schematically in Figure (2). The

Surface area	1122.13 (m <sup>2</sup> / g)
Bulk density	0.4423 (g /cm <sup>3</sup> )
Porosity	0.48972 (-)

test section consists of a cylindrical column of (7.5) cm inside diameter and (50) cm height filled to a height of 24 cm with (400) g activated carbon (dp=1-3 mm). The chemical analysis and the physical properties of the activated carbon used in this study were given in tables (1 and 2), respectively. The chemical analysis was determined using atomic absorption, and the physical properties were obtained using surface area analyzer. A (T-type) thermocouple was used to measure the temperature of the activated carbon bed. The thermocouple was connected to an on/off controller to adjust the bed temperature. A heater of 225 watt, wrapped around the bed, was used to heat the bed to the required temperature. The heater was connected to a variac that regulates the electrical current supplied to the heater.

**Table (1): Chemical Analysis of Activated Carbon**

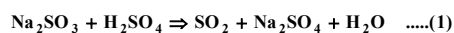
Material	wt %	Material	wt %
C	92.46	Mg <sup>+2</sup>	3.25
Ca <sup>+2</sup>	2.75	Mn <sup>+2</sup>	0.116

Co <sup>+2</sup>	0.075	Pb <sup>+2</sup>	0.512
Cu <sup>+2</sup>	0.15	PO <sub>4</sub> <sup>-3</sup>	0.018
Fe <sup>+2</sup>	0.0696	SO <sub>4</sub> <sup>-2</sup>	0.018
Fe <sup>+3</sup>	0.325	Zn <sup>+2</sup>	0.025

**Table (2): Physical Properties of Activated Carbon**

### • Experimental Procedure:

Four hundreds grams of (1-3) mm particles diameter of activated carbon were introduced into the test section. A slurry of activated carbon was prepared by immersing the activated carbon bed with 2 liter of water. Sulfur Dioxide gas was synthesized <sup>(7)</sup> by dropping the desired concentration of sulfuric acid into the SO<sub>2</sub> generation flask that contains the aqueous sodium sulfite solution according to the chemical reaction:



After adjusting the bed temperature to the desired value, the air stream at a desired flow rate was then passed through this container to carry the SO<sub>2</sub> to the test section. The initial concentration of SO<sub>2</sub> was measured at the beginning of each run. In order to measure the concentration of SO<sub>2</sub> in the effluent gas stream, (10) ml of the iodine sample was taken from the absorption trap, titrated with standard sodium thiosulfate solution (0.1) N, in the presence of starch indicator.

This step was repeated every 5 minutes till the end of experimental run time (1 hr). After each experimental run the bed was washed with fresh water until the concentration of SO<sub>2</sub> gas in the air stream is free from SO<sub>2</sub>. Each experimental run were repeated for 3-5 times to validate the experimental results. The removal efficiency of SO<sub>2</sub> was calculated as the ratio of SO<sub>2</sub> concentration that was adsorbed by activated carbon to the initial concentration of SO<sub>2</sub> gas fed to the bed.

$$\eta(\%) = \frac{C_0 - C_{SO_2}}{C_0} * 100 \quad \text{.....(2)}$$

### 3- Model Development

The following assumptions were used to formulate the mathematical model: constant porosity, spherical solid particle, dispersion radial and axial directions are neglected (i.e. plug flow), and isothermal process.

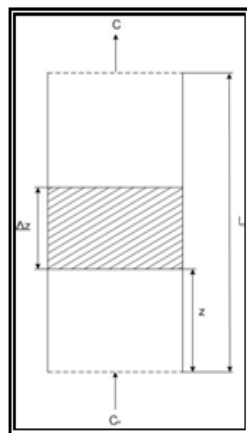


Figure (1) Mathematical Representation of the Model

#### - For The Gas Phase

Referring to Figure (1) a mass balance is performed for the gas phase:-

$$\left[ \begin{matrix} \text{molar rate} \\ \text{In} \end{matrix} \right] - \left[ \begin{matrix} \text{molar rate} \\ \text{out} \end{matrix} \right] - \left[ \begin{matrix} \text{molar rate of} \\ \text{disappearance} \end{matrix} \right] = \left[ \begin{matrix} \text{molar rate of} \\ \text{accumulation} \end{matrix} \right] \quad \text{.....(3)}$$

$$F_{SO_2}|_z - F_{SO_2}|_{z+\Delta z} - a r_{SO_2} (A_R \Delta z) = \varepsilon \rho (A_R \Delta z) \frac{\partial C_{SO_2}}{\partial t} \quad \text{.....(4)}$$

Dividing both sides by  $(A_R \Delta z)$  and taking the limit as  $\Delta z \rightarrow 0$

$$\lim_{\Delta z \rightarrow 0} \frac{F_{SO_2}|_z - F_{SO_2}|_{z+\Delta z}}{A_R \Delta z} - a r_{SO_2} = \varepsilon \rho \frac{\partial C_{SO_2}}{\partial t} \quad \text{.....(5)}$$

$$- \frac{\partial F_{SO_2}}{A_R \partial z} - a r_{SO_2} = \varepsilon \rho \frac{\partial C_{SO_2}}{\partial t}$$

$$\frac{F_{SO_2}}{A_R} = u C_{SO_2} \quad \left( \frac{\text{mol}}{\text{m}^2 \text{ s}} = \frac{\text{m}}{\text{s}} \cdot \frac{\text{mol}}{\text{m}^3} \right) \quad \text{.....(6)}$$

$$- u_z \frac{\partial C_{SO_2}}{\partial z} - a r_{SO_2} = \varepsilon \rho \frac{\partial C_{SO_2}}{\partial t}$$

Transfer the differential equation into dimensionless form:

$$- \frac{C_0 u_z}{L} \frac{\partial \frac{C_{SO_2}}{C_0}}{\partial \frac{z}{L}} - a r_{SO_2} = \varepsilon \rho C_0 \frac{\partial \frac{C_{SO_2}}{C_0}}{\partial t} \quad \text{.....(7)}$$

$$Z = \frac{z}{L}$$

$$Y = \frac{C_{SO_2}}{C_0}$$

$$n = C_o u_z A_R \left( \frac{\text{mol}}{\text{s}} = \frac{\text{mol}}{\text{m}^3} \cdot \frac{\text{m}}{\text{s}} \cdot \text{m}^2 \right) \quad \text{.....(8)}$$

$$-\frac{n}{A_R L} \frac{\partial Y}{\partial Z} - a r_{\text{SO}_2} = \varepsilon \rho C_o \frac{\partial Y}{\partial t} \quad \text{.....(9)}$$

$$a = \frac{S_e w}{V_R}$$

Rearranging equation (9) gives:

$$\frac{n}{L A_R} \frac{\partial Y}{\partial Z} + \frac{S_e w}{V_R} r_{\text{SO}_2} + \varepsilon \rho C_o \frac{\partial Y}{\partial t} = 0 \quad \text{.....(10)}$$

### - For the Solid Phase:-

Referring to Figure (1) a mass balance is performed for the solid phase:-

$$\left[ \begin{array}{c} \text{molar rate} \\ \text{In} \end{array} \right] - \left[ \begin{array}{c} \text{molar rate} \\ \text{out} \end{array} \right] - \left[ \begin{array}{c} \text{molar rate of} \\ \text{disappearance} \end{array} \right] = \left[ \begin{array}{c} \text{molar rate of} \\ \text{accumulation} \end{array} \right] \quad \text{.....(3)}$$

$$-(-r_{\text{SO}_2}) v_s S_e M = \frac{\partial (C_o - C_{\text{SO}_2})}{\partial t} \quad \text{.....(11)}$$

$$\frac{(C_o - C_{\text{SO}_2})}{C_o} = X \text{ (Sorbent Conversion)}$$

Rearranging equation (4 - 3) gives :

$$\frac{\partial X}{\partial t} = r_{\text{SO}_2} v_s S_e M \quad \text{.....(12)}$$

To solve equations (10) and (12) the following initial boundary conditions are used:

$$a - \text{at } t = 0 \text{ \& } Z > 0 \Rightarrow Y = 0, X = 0$$

$$b - \text{at } Z = 0 \text{ \& } t > 0 \Rightarrow Y = 1$$

In order to solve the differential equations (10) and (12) a rate expression of the desulfurization reaction,  $\text{SO}_2$  was assumed to react with water molecules in the presence of the sorbent to form  $\text{H}_2\text{SO}_3$  according to the reaction:



The rate of reaction ( $r_{\text{SO}_2}$ ) for the desulfurization reaction over the sorbent can be expressed as a product of a temperature dependent rate constant  $k(T)$  and the concentration of the reactants <sup>(36)</sup> as shown:

$$r_{\text{SO}_2} = \frac{dX}{dt} = k(T) [\text{SO}_2]^\alpha [\text{H}_2\text{O}]^\beta \quad \text{.....(14)}$$

Where ( $\alpha$ ) is the order of the reaction with respect to  $\text{SO}_2$  and ( $\beta$ ) is the order of the reaction with respect to  $\text{H}_2\text{O}$ . Assuming that the concentration of  $\text{H}_2\text{O}$  is in excess as compared to  $\text{SO}_2$ , Eq. (14) can be simplified to:

$$\frac{dX}{dt} = k(T) C_o (1 - X)^\alpha (\text{RH})^\beta \quad \text{.....(15)}$$

Where ( $C_o$ ) is the initial concentration of  $\text{SO}_2$  and ( $\text{RH}$ ) is the relative humidity of the feed gas.

The temperature dependent rate constant in Eq. (15) is taken as the global reaction rate constant which obeys the Arrhenius Law <sup>(12)</sup>,  $k$ , given by:

$$k(T) = k = A_f \exp\left(-\frac{E}{RT}\right) \quad \text{.....(16)}$$

Where ( $E$ ) is the activation energy of the desulfurization reaction, ( $A_f$ ) is the frequency or pre-exponential factor of the desulfurization reaction and ( $R$ ) is the universal gas constant. The rate expression for the desulfurization reaction can be written as:

$$r_{so_2} = A_f \exp\left(-\frac{E}{RT}\right) C_o (1-X)^\alpha (RH)^\beta \quad \text{.....(17)}$$

With the inclusion of effectiveness factor ( $\xi$ ) in the rate expression, it is written as:

$$r_{so_2} = \xi A_f \exp\left(-\frac{E}{RT}\right) C_o (1-X)^\alpha (RH)^\beta \quad \text{.....(18)}$$

The effectiveness factor is taken as a constant equal to 0.9. In order to obtain the values of ( $A_f$ ,  $\alpha$ ,  $E$  and  $\beta$ ) Eq. (18) was substituted into Eq. (10) and Eq. (12), yielding Eqs.(19) and Eq. (20).

**For the gas phase:-**

$$\frac{n}{L A_R} \frac{\partial Y}{\partial Z} + \varepsilon \rho C_o \frac{\partial Y}{\partial t} + \frac{S_e w}{V_R} \left[ \xi A_f \exp\left(-\frac{E}{RT}\right) C_o (1-X)^\alpha (RH)^\beta \right] = 0 \quad \text{.....(19)}$$

**For the solid phase:-**

$$\frac{\partial X}{\partial t} = v_s S_e M \left[ \xi A_f \exp\left(-\frac{E}{RT}\right) C_o (1-X)^\alpha (RH)^\beta \right] \quad \text{.....(20)}$$

The ordinary differential equation was solved numerically. The values of ( $A_f$ ,  $\alpha$ ,  $E$  and  $\beta$ ) were then obtained by least-square fitting of the solved ordinary differential equation to the experimental data.

A computer program has been developed in Matlab V7.0 to perform the numerical solution formulated previously. The values of  $A_f$ ,  $\alpha$ ,  $E$  and  $\beta$  were found to be 1.07, 2.2, 25 kJ/mol and 3.1 respectively.

#### 4- Results & Discussion

Figure (3) clarify that an optimal overall removal efficiency can be obtained at gas rate of 60 l/min. Beyond this value the overall removal efficiency decreases. These results are in agreement with the work of Liu et al. <sup>(6)</sup> who obtained a similar behavior for the change of space velocity with SO<sub>2</sub> removal efficiency. This may be attributed to that the kinetic behavior varied with gas rate and the desulfurizing property was controlled by diffusion at gas rates less than 60 l/min., and controlled by adsorption or catalytic reaction at gas rates higher than 60 l/min.

Figure (4) shows the change of the overall removal efficiency of SO<sub>2</sub> with temperature for different initial SO<sub>2</sub> concentrations, and constant flue gas flow rate of 20 l/min in wet bed conditions. The trend of the results indicate that the overall removal efficiency is independent of SO<sub>2</sub> initial concentration at low temperatures ( $T=30$  and  $40$ ) °C and increases at higher temperatures. The significantly higher activity of the surfaces of the adsorbents carbonized at higher temperature result from the combined effect of dehydroxylation of inorganic phase oxides and their solid state reactions promoted at high temperature and reducing conditions and with increasing temperature new reactive oxides formed, e.g. FeSO<sub>3</sub> and/or CaSO<sub>3</sub> are well-developed compared to the starting material.

Figure (5) shows the effect of temperature on the overall removal efficiency of  $\text{SO}_2$  for constant flue gas flow rate of 20 l/min in dry bed conditions. The trend of the results shows a similar pattern as that obtained in wet bed where at low temperatures the effect of the initial concentration of  $\text{SO}_2$  is minimal and increases as the temperature increases. In dry beds, the absence of water precludes the formation of sulfuric acid in the pore system. However, it is possible that at higher temperatures  $\text{SO}_2$  forms sulfites through reactions with oxides to form  $\text{FeSO}_4$  and/or  $\text{CaSO}_3$  that are not formed at lower temperatures.

Figures (6) to (9) show the effect of initial concentrations of  $\text{SO}_2$  for an hour interval on the effluent concentration of  $\text{SO}_2$  at constant flow rate 20 l/min, and various temperatures in wet and dry bed conditions. The results indicate that at any certain time the effluent concentration of  $\text{SO}_2$  increases as the initial concentrations of  $\text{SO}_2$  increases. This is due to the decrease in the activity of activated carbon as a direct consequence of exposing a fixed amount of the sorbent to the increasing concentration of  $\text{SO}_2$ .

Figures (10) to (13) show the change of effluent concentration with time for wet and dry bed conditions for an hour interval at constant flue gas rate of 20 l/min, and different operating conditions. The trends of the results indicate a lower value for the

effluent gas concentration in the wet beds as compared to those in dry beds for the same experimental conditions. Moreover the difference in the concentration of  $\text{SO}_2$  in the effluent gas between wet and dry bed conditions at any time becomes higher as the temperature of the bed increased. Bagreev and Bandoz<sup>(5)</sup> explained that for high temperature, volume decreases in micropores, which indicates the gradual filling of these pores with the products of surface reactions (assuming that  $\text{SO}_2$  is oxidized to  $\text{H}_2\text{SO}_4$  of density 1.83 g/cm<sup>3</sup> in wet bed and suggests that the acid is deposited at entrances to the pores). Therefore in the presence of water, the removal of  $\text{SO}_2$  is much larger than that for dry bed.

Figure (14) shows the break-through life of 200 g of the activated carbon at flue gas flow rate of 60 l/min, initial concentration of  $\text{SO}_2$  of 500 ppm and a temperature of 80 °C in wet bed. From the curve obtained, it can be seen that the effluent concentration of  $\text{SO}_2$  increases with time until a time of about 600 min beyond which the concentration of the activated carbon bed with time<sup>(10)</sup>.

Figure (15) shows the simulated vs. experimental curves at two different experimental conditions. It can be seen that the model gives very good predications for the experimental data. The confidence level of the model

was 95% using the goodness of fit test <sup>(11)</sup>.

### 5- Conclusions:

The conclusions withdrawn from the present study may be summarized as follows: The removal efficiency of SO<sub>2</sub> increased on increasing the flue gas flow rate till 60 l/min and then decreases slowly. The removal efficiency depends on the reaction temperature to a large extent. The results indicate an increase in the SO<sub>2</sub> removal efficiency of about 3.6% on increasing the temperature by 10 °C in the range of (30-60) °C and an increases of about 1.7% in the range of (60-80) °C, all for 1 hr and C<sub>0</sub>=500 ppm in wet bed.

A reduction in the SO<sub>2</sub> removal efficiency was observed on increasing the SO<sub>2</sub> initial concentration in the flue gas stream. The removal efficiency of SO<sub>2</sub> was higher under wet conditions than that under dry conditions. The mathematical model proposed was found to provide a good description of the desulfurization reaction under conditions prevailing in the flue gas desulfurization process at higher temperature.

### References:-

1. Lizzio, A., A., and DeBarr, J., A., "Mechanism of SO<sub>2</sub> Removal by Carbon", *Energy Fuels*, 11, (2), 284-291, 1997.
2. Cho, E., H., "Removal of SO<sub>2</sub> with Oxygen in The Presence of Fe (III)", *Met. Trans. B*, (17B), 745-753, 1986.
3. Bagreev, A., Bashkova, S., Locke, D., C., and Bandosz, T., J., "Sewage Sludge – Derived Materials as Adsorbents of SO<sub>2</sub>", *Environ. Sci. Technol.*, 35 (15), 3262-3289, 2001.
4. Cho, E., H., and Miller, H., L., "SO<sub>2</sub> Removal with Coal Scrubbing", M.Sc. Thesis, University of West Virginia, 2002.
5. Bagreev, A., and Bandosz, T., J., "The Role of Water in the Process of Methyl Mercaptans Adsorption on Activated Carbons", *Carbon Conference*, Spain, 2003.
6. Liu, Q., Li, C. and Li, y., "SO<sub>2</sub> Removal from Flue Gas by Activated Semi-Cokes 1.The Preparation of Catalysts and Determination of Operating Conditions", *Carbon*, 12, (41), 2217-2223, 2003.
7. Lippert, B., P., Stejskalora, K., and Mocek, K., *Chemike Listy*, (88), 60-61, 1994.
8. Fogler, H., S., "Element of Chemical Engineering", 2nd Ed., Mc-Graw Hill, New York, 1984.

9. Smith, J., M., and Van Ness, H., C., "Introduction to Chemical Engineering Thermodynamics", 4<sup>th</sup> Ed., New York, 300, 2000.
10. Treybal, R., E., "Mass Transfer Operation", 3<sup>rd</sup> Ed., Mc-Graw Hill, New York, 1981.
11. Subhi, M., and Awad, A., "Introduction to Statistics", 1<sup>st</sup> Ed., Jordanian Book Center, Amman, 1990.

### Nomenclature

Symbol	Definition	Unit
$A_R$	Transversal bed section	$m^2$
$a$	Specific area of the bed	$m^2/m^3$
$A_f$	Frequency factor	$s^{-1}$
$C_0$	Initial conc.of $SO_2$	ppm
$C_{SO_2}$	Effluent conc.of $SO_2$	ppm
$C$	$SO_2$ conc.	ppm
$d_p$	Slurry particle diameter	mm
$E$	Activation energy	$kJ.mol^{-1}$
$k$	Global reaction rate constant	$s^{-1}$
$k(T)$	rate constant	$s^{-1}$
$L$	Bed length	m
$M$	Molecular weight of activated carbon	$g.mol^{-1}$
$n$	Molar flow rate of $SO_2$	$mol.s^{-1}$
$Q$	Flow rate of $SO_2$	l/min
$R$	Universal gas constant	$J.mol^{-1}.K^{-1}$
$RH$	Relative humidity	[%]
$r_{SO_2}$	Reaction rate	$mol.m^{-2}.s^{-1}$
$S_e$	Specific surface area	$m^2.g^{-1}$
$T$	Temperature	$^{\circ}C$
$t$	Time	s or min
$u$	Axial superficial velocity of gas	$m.s^{-1}$
$v_s$	Stoichiometric coefficient	[-]
$V_{STP}$	Volume of gas at standard conditions	$\ell$
$V_R$	Volume of the reaction bed	$m^3$
$w$	Sorbent weight in the bed	g
$X$	Sorbent conversion	[-]
$Y$	Dimensionless $SO_2$ concentration ( $C/C_0$ )	[-]
$Z$	Dimensionless length position	[-]
$\alpha$	Order of the desulfurization reaction with respect to $SO_2$	[-]
$\beta$	Order of the desulfurisation reaction with respect to $H_2O$	[-]
$\rho$	Molar density of solid particles	$[mol.m^{-3}l.m^{-3}]$
$\eta$	Removal efficiency of $SO_2$	[%]
$\varepsilon$	Bed porosity	[-]

$\eta$	Removal efficiency of $\text{SO}_2$	[%]
$\xi$	Effectiveness factor	[-]

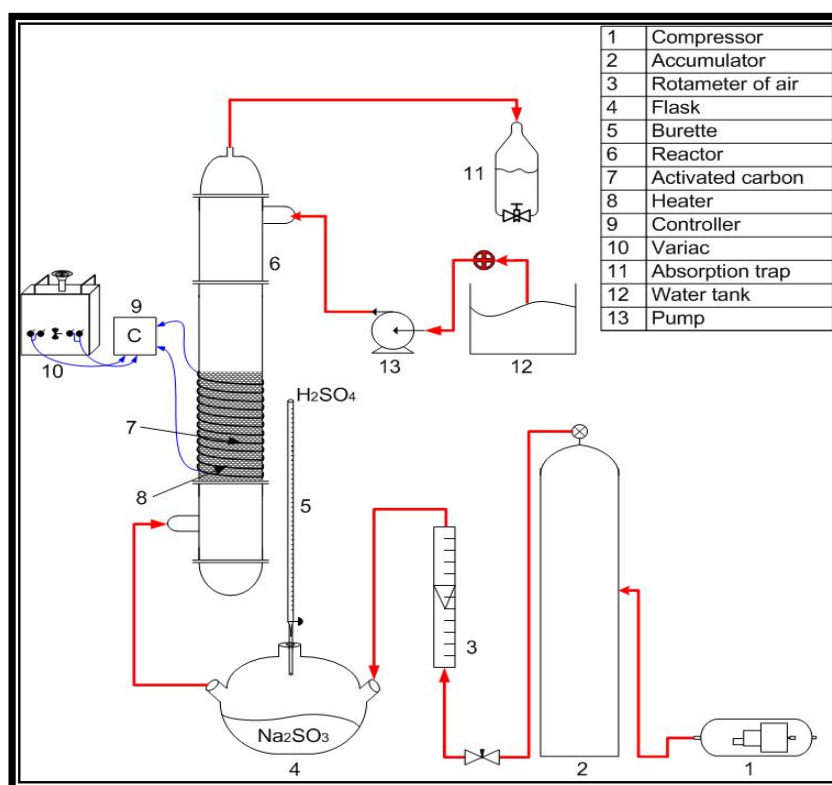
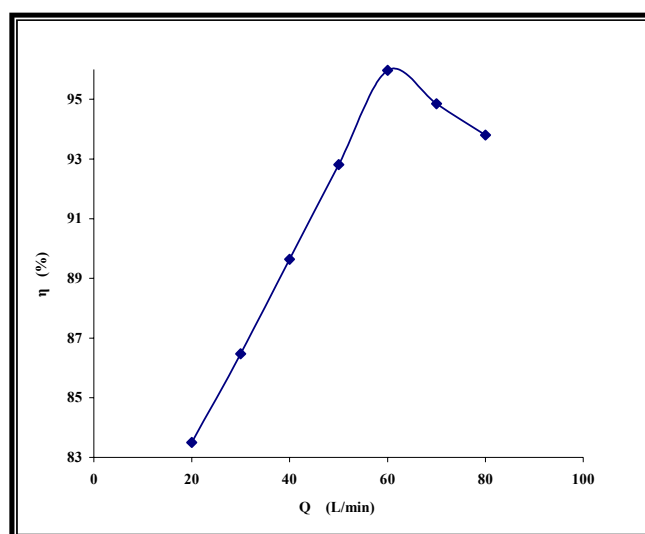


**Figure (2) Schematic Diagram of the Experimental Set-up**



\* Dept. Chemical Eng., Univ. of Tech.

**Figure (3) The effect of gas flow rate on the overall removal efficiency of  $\text{SO}_2$  in wet bed**

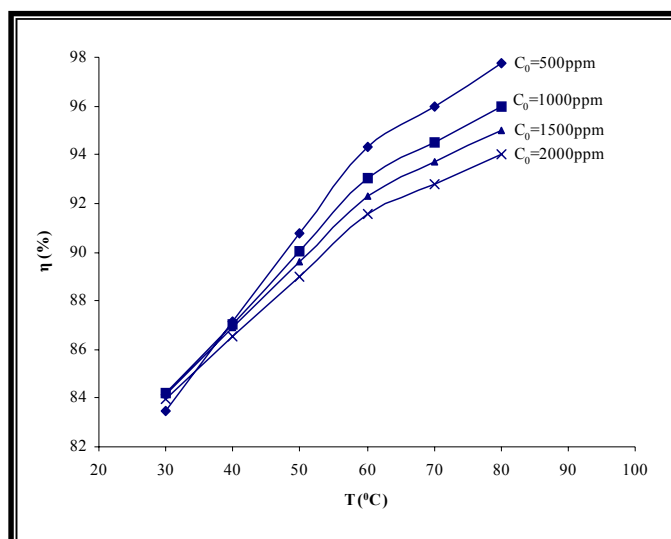


**Figure (4) The effect of temperature on the overall removal efficiency of sulfur dioxide at  $Q=20$  l/min in wet bed**

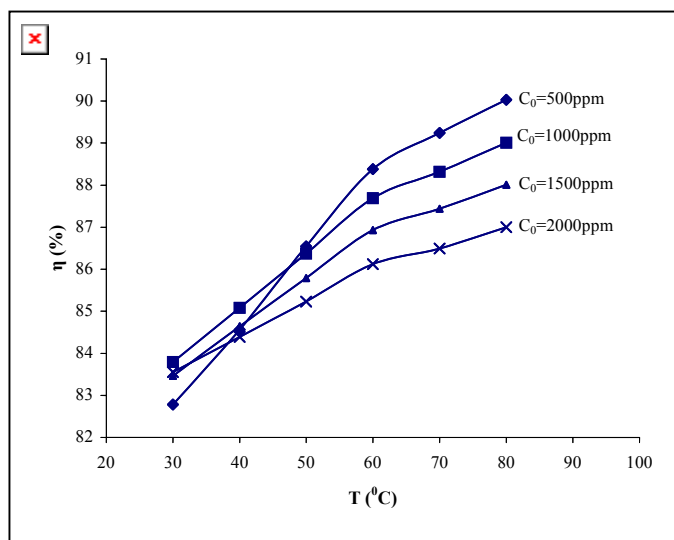


**Figure (5) The effect of temperature on the overall removal efficiency of sulfur dioxide at  $Q=20$  l/min in dry bed**

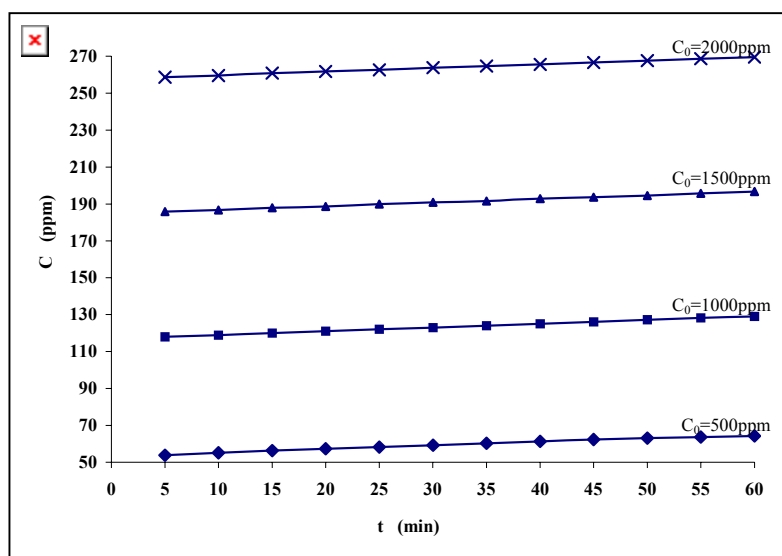


**Figure (6) The effect of  $SO_2$  initial concentration on the effluent concentration of  $SO_2$  ( $T=40^\circ C$ ) in wet bed condition**

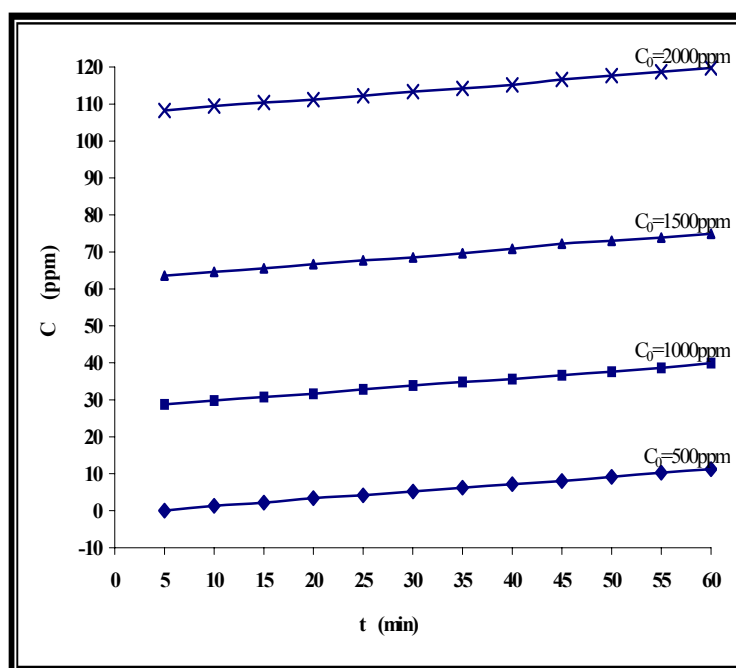


**Figure (7) The effect of  $SO_2$  initial concentration on the effluent concentration of  $SO_2$  ( $T= 80 ^\circ C$ ) in wet bed condition**

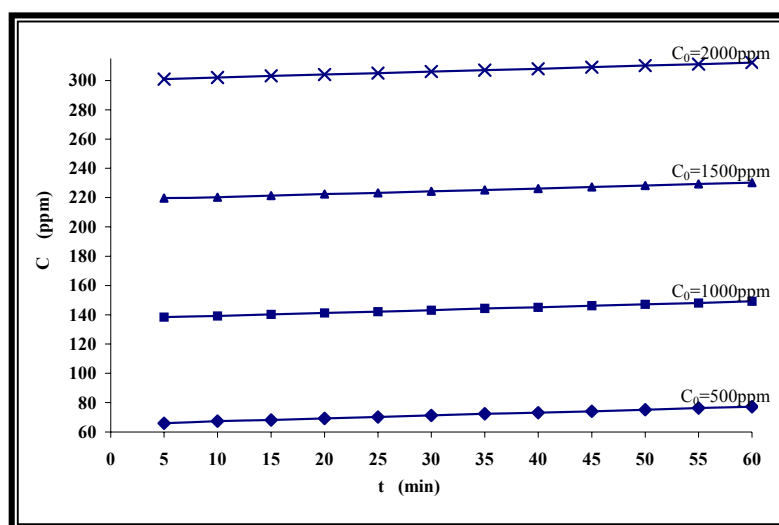


**Figure (8) The effect of  $SO_2$  initial concentration on the effluent concentration of  $SO_2$  ( $T= 40 ^\circ C$ ) in dry bed condition**

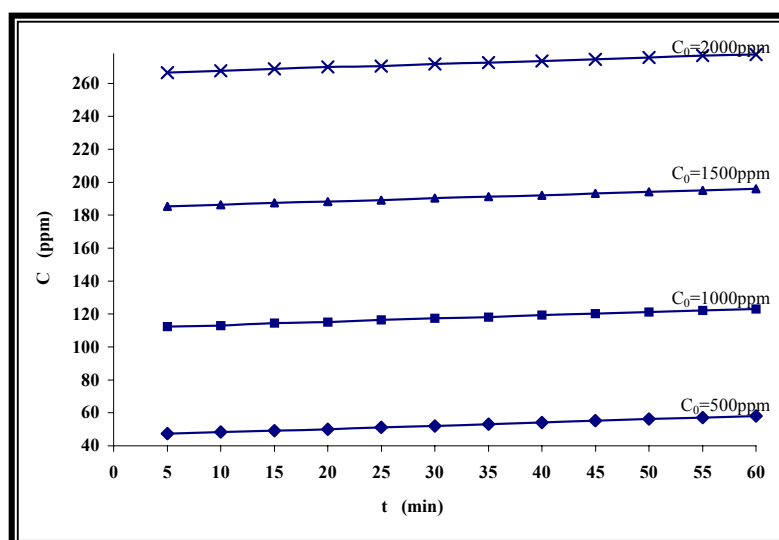


**Figure (9) The effect of  $SO_2$  initial concentration on the effluent concentration of  $SO_2$  ( $T= 80 ^\circ C$ )**

*in dry bed condition*

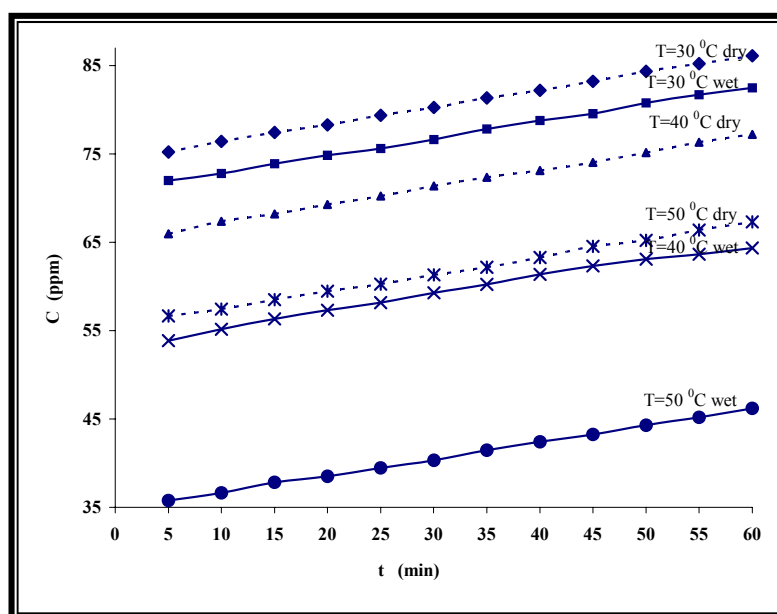


**Figure (10) The effect of wet and dry conditions on the effluent concentration of  $\text{SO}_2$  ( $T=30, 40 \text{ \& } 50^\circ\text{C}$ ),  $C_0=500\text{ppm}$**

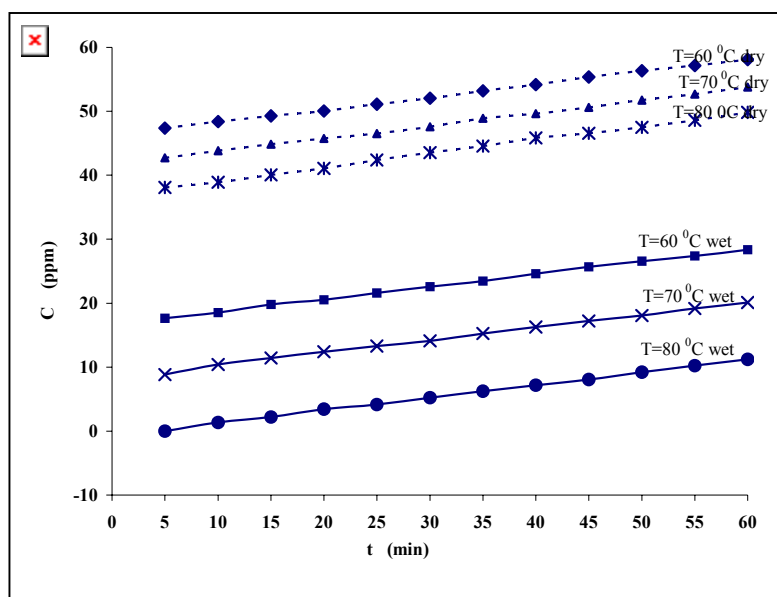


**Figure (11) The effect of wet and dry conditions on the effluent concentration of  $SO_2$  ( $T=60, 70$  &  $80$ )  $^{\circ}C$ ,  $C_0=500ppm$**

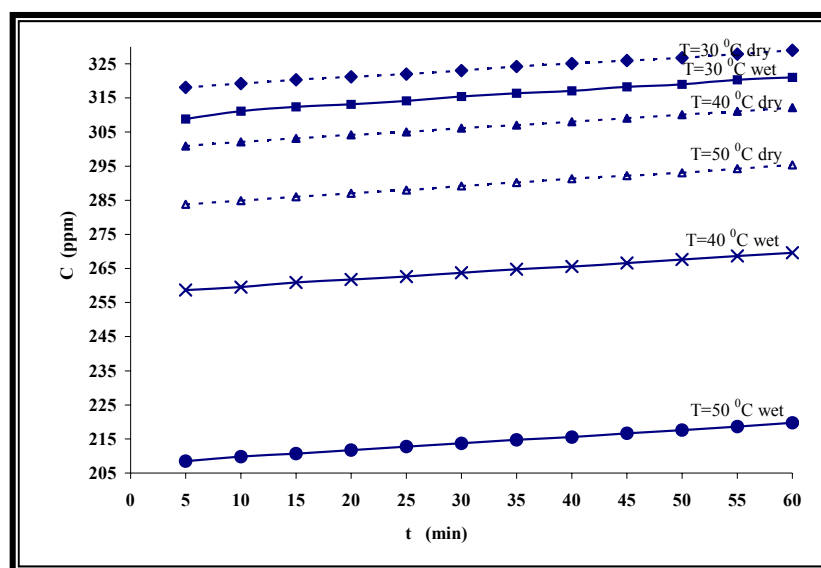


**Figure (12) The effect of wet and dry conditions on the effluent concentration of  $SO_2$  ( $T=30, 40$  &  $50$   $^{\circ}C$ ),  $C_0=2000ppm$**

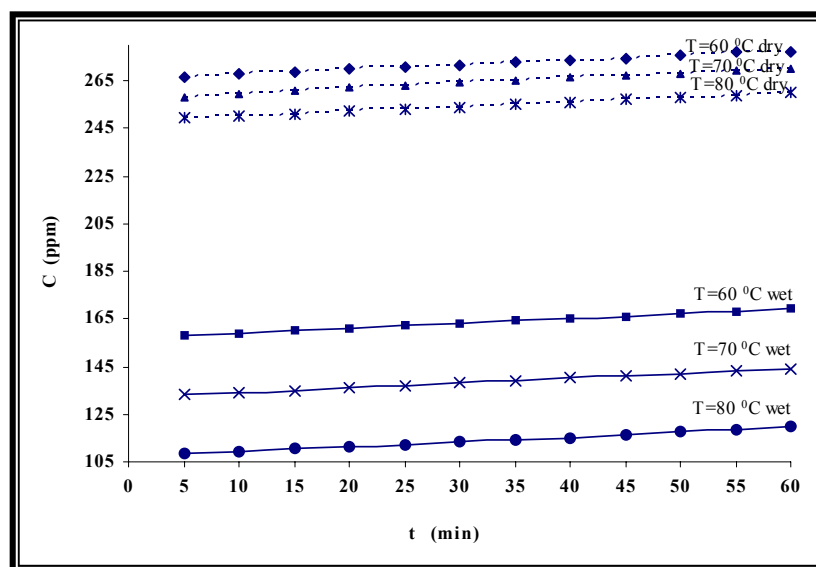


**Figure (13) The effect of wet and dry conditions on the effluent concentration of  $SO_2$  ( $T=60,70$  &  $80^\circ C$ ),  $C_0=2000ppm$**

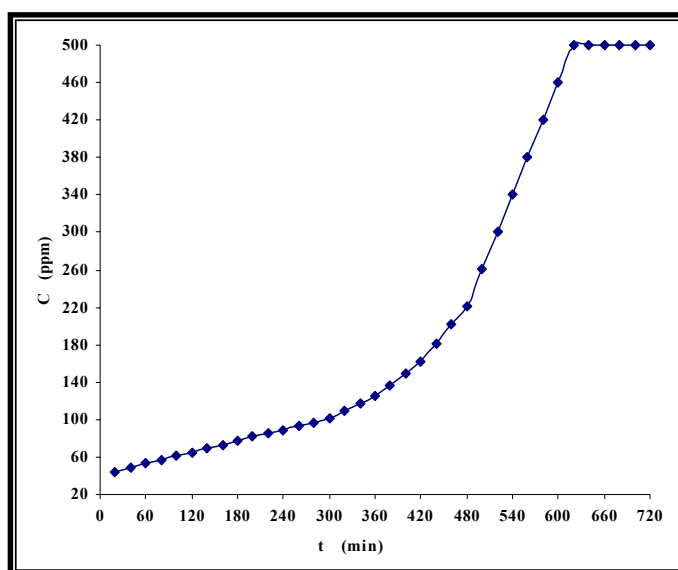


**Figure (14) The breakthrough life of 200g of activated carbon at  $Q=60$  l/min,  $C_0=500$  ppm and  $T=80^\circ C$  in wet bed**

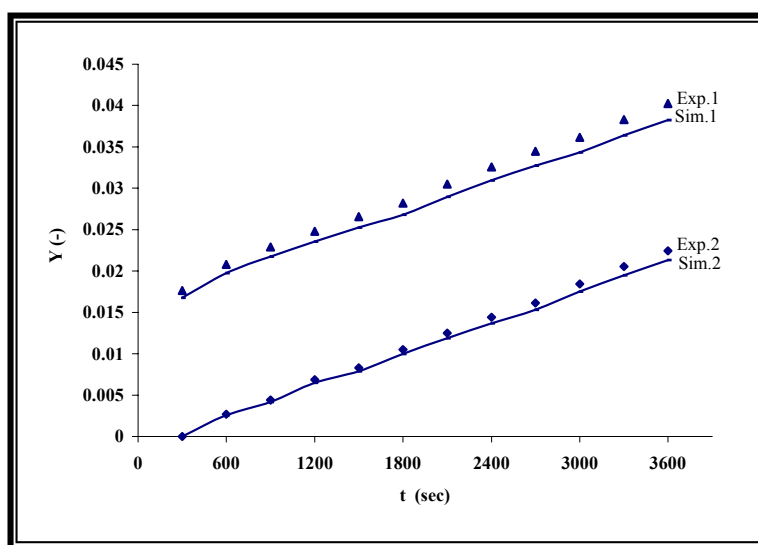


***Figure (15) Comparison between simulated  
and experimental results for:***

***Condition1:  $C_0=500\text{ppm}$ ,  $T=70^\circ\text{C}$  in wet bed***

***Condition2:  $C_0=500\text{ppm}$ ,  $T=80^\circ\text{C}$  in wet bed***